

NASA Contractor Report 172259

POSTOP: Postbuckled Open- Stiffener Optimum Panels- Theory and Capability

J. N. Dickson

S. B. Biggers

LOCKHEED-GEORGIA COMPANY
A Division of Lockheed Corporation
Marietta, Georgia

Contract NAS1-15949
January 1984



National Aeronautics and
Space Administration

Langley Research Center
Hampton, Virginia 23665

FOREWORD

This report is prepared by the Lockheed-Georgia Company under Contract NAS1-15949, "Advanced Composite Structural Design Technology for Commercial Transport Aircraft," and describes the theory and capability of a computer program prepared for the analysis and sizing of stiffened composites panels. This work was performed under Task Assignment No. 5 of the contract. The program is sponsored by the National Aeronautics and Space Administration, Langley Research Center (NASA/LaRC). Dr. James H. Starnes is the Project Engineer for NASA/LaRC. John N. Dickson is the Program Manager for the Lockheed-Georgia Company.

In addition to the authors the following Lockheed specialist/consultants made major contributions to the material presented.

L.W. Liu

Programming

Dr. J.T.S. Wang (Georgia Tech.)

Analysis

TABLE OF CONTENTS

	Page
SUMMARY	1
INTRODUCTION	1
SYMBOLS	3
STRUCTURAL ANALYSIS	7
Section Properties and Panel Stiffnesses	7
Beam-Column Analysis	11
Rotational Restraint of Skin	15
Postbuckled Plate Analysis	18
Average stress resultants	
Initial buckling of skin	
Strains in postbuckled skin	
Buckled skin stiffnesses	
Design Strain limitations	24
Stiffener Strength	25
Stiffener Local Buckling	25
Rolling of Stiffeners	27
Torsional/Flexural Buckling of Stiffeners	29
Calculation of membrane forces acting on stiffener	
Effect of skin bending on stiffener buckling	
Formulation of stability matrix	
Skin/Stiffener Interface Stress Analysis	38
Skin Layup Design Constraints	43
Multiple Load Cases	44
SIZING	45
Optimization Problem Statement	45
Optimization Procedure	46
REFERENCES	47

POSTOP: Postbuckled Open-STiffener Optimum Panels - Theory and Capability

John N. Dickson and Sherrill B. Biggers
Lockheed-Georgia Company
Marietta, Georgia

SUMMARY

A computer program, POSTOP, for the analysis or sizing of stiffened panels is described. Buckling resistant or postbuckled panels subject to loading conditions typical of aerospace structures may be treated. Composite materials may be used. Analytical routines are included to compute panel stiffnesses, strains, local and panel buckling loads, and skin/stiffener interface stresses. Multiple load cases may be defined. Sizing is performed by the COPES/CONMIN optimization routines. This report describes the analytical and sizing procedures used in the program.

INTRODUCTION

Stiffened panels are widely used in aerospace structures. Applications include fuselages, lifting and control surfaces, spar webs, bulkheads and floors among others. The skin or web is typically required to remain unbuckled under some loading conditions but allowed to enter the postbuckling regime under other more severe loading conditions. For example, metal transport fuselages are normally allowed to buckle at ultimate loads but are required to be unbuckled at loads corresponding to 1g. level flight. The preliminary design of minimum-weight stiffened panels subject to multiple loading conditions and various requirements associated with each loading condition can become a formidable problem. If composite materials are to be considered, the number of design variables and the size of the optimization problem, as well as the complexity of the required analyses, may increase substantially.

As an aid to the preliminary design of stiffened composite panels that may be loaded in the postbuckling regime, an analysis and sizing code, POSTOP, has been developed. A comprehensive set of analysis routines has been coupled to the COPES/CONMIN (Reference 1) optimization program to produce this sizing code. POSTOP is intended for the preliminary design of metal or composite panels with open-section stiffeners, subjected to combined biaxial compression (or tension), shear and normal pressure loading. Longitudinal compression, however, is assumed to be the dominant loading. Temperature, initial bow eccentricity and load eccentricity effects are included. The panel geometry is assumed to be repetitive over several bays in the longitudinal (stiffener) direction as well as in the transverse direction. These restrictions were imposed to allow the development of analysis routines with the efficiency required in a practical sizing code. The resulting program is applicable to stiffened panels as commonly used in fuselage, wing, or empennage structures.

This report describes in some detail the analysis procedures and rationale for the assumptions used therein. A brief description of the sizing methodology is given. Further discussions of the optimization procedure and routines are available in References 1-3. Detailed instructions for the use of the code and interpretation of the output from the program are given along with several examples in a separate User's Manual (Reference 4).

SYMBOLS

Symbols generally are defined in the text as they first occur. A list of the more important ones is given below.

a_{ij}	- tangent in-plane stiffnesses of postbuckled plate
b_s	- stiffener spacing
k_{sk}	- rotational stiffness of skin used in stiffener local buckling analysis
p	- normal pressure load
u, v, w	- longitudinal, transverse and normal displacements of a plate
u^o, v^o, w^o	- x, y, and z direction displacements of stiffener shear center
x, y, z	- coordinate directions
y_o, z_o	- stiffener shear center coordinates relative to centroid
$\bar{y}_{ST}, \bar{z}_{ST}$	- stiffener centroid coordinates
y_L, y_R, z_R	- coordinates of lines where skin attaches to stiffener in torsional/flexural analysis
\bar{z}_i	- vertical distance from panel centroid to i^{th} stiffener element
A_{ij}	- plate in-plane stiffnesses
\bar{A}_{xi}	- longitudinal extensional stiffness of i^{th} stiffener element

- $A_{xsk}^{tan}, A_{xsk}^{sec}$ - tangent and secant longitudinal extensional stiffness of postbuckled plate
- D_{ij} - plate bending stiffnesses
- \bar{D}_{xi} - longitudinal bending stiffness of i^{th} stiffener element
- EA_x - panel longitudinal extensional stiffness
- EI_y - panel longitudinal bending stiffness
- EA, GJ, C_1 - stiffener extensional, torsional and warping stiffnesses
- $EI_{yy}, EI_{yz}, EI_{zz}$ - stiffener bending stiffnesses
- EA_S, EA_T - secant and tangent panel extensional stiffnesses
- EI_S, EI_T - secant and tangent panel bending stiffnesses
- EI_O - stiffener polar bending stiffness
- $G_j(X_i)$ - j_{th} constraint
- K_θ, K_ϕ - rotational stiffness of stiffener, equations 21 and 23
- K_R - net rotational stiffness of stiffener, equation 24
- $M_{yy}^{(k)}, V_y^{(k)}$ - transverse moment and normal shear constraints on k^{th} stiffener
- M_E, M_N, M_P - moments due to bow eccentricity, axial load eccentricity and pressure
- MS_j - margin of safety for failure mode j

- N_x, N_y, N_{xy} - applied longitudinal, transverse and shear loads
- N_{xi} - longitudinal stress resultant in i^{th} stiffener element
- $N_{yy}^{(k)}, N_{xy}^{(k)}$ - in-plane transverse and shear constraint forces on k^{th} stiffener
- N_1, N_2, N_{12} - average longitudinal, transverse and shear stress resultants on post-buckled plate
- N^T - equivalent thermal loads
- N_{xi}^T - equivalent longitudinal thermal loads in i^{th} stiffener element
- N_{ni}^T, N_{ysk}^T - equivalent transverse thermal loads in i^{th} stiffener element and skin
- P_E, \bar{P}_E - standard and modified Euler loads
- \bar{P} - stiffener compression load
- P_n - n^{th} degree Legendre polynomial
- R_y, R_z - reaction forces on stiffener at center of rotation
- V - strain energy per unit area of postbuckled plate
- w_i - width of i^{th} stiffener element, $i = 1, 5$
- x_i - i^{th} design variable
- $Y(X_i)$ - objective function
- ϵ - laminate strains

- ϵ_{xi} - longitudinal strain in i^{th} stiffener element
- $\epsilon_1, \epsilon_2, \gamma_{12}$ - longitudinal, transverse and shear strains at edges of postbuckled plate
- θ - rotation of stiffener, flexible cross-section
- κ_x - longitudinal curvature of panel
- λ - half-wavelength
- ν_{xi}, ν_{xysk} - Poisson's ratio in i^{th} stiffener element and skin
- ϕ - rotation of stiffener, rigid cross-section
- $\sigma_x, \sigma_y, \sigma_z$ - longitudinal, transverse and normal stresses at skin/stiffener interface
- $\tau_{xy}, \tau_{xz}, \tau_{yz}$ - in-plane and transverse shear stresses at skin/stiffener interface

STRUCTURAL ANALYSIS

A flow chart of the principal elements of the analyses is shown in Figure 1. Initially skin/stiffener section properties are calculated assuming the skin to be unbuckled to obtain a first estimate of the longitudinal strain and curvature of the panel. Since the rotational restraint provided by the stiffener to the skin is a function of the stiffener load, it may be determined only after the panel strain and curvature are known. If the applied loads cause buckling of the skin (assuming skin buckling is permitted), the postbuckled plate analysis is performed and an iterative procedure is needed to determine the correct strain and curvature of the panel. The postbuckled plate analysis provides the tangent and secant stiffnesses of the buckled skin needed in determining the panel strain and curvature. The rotational restraint of the skin by the stiffener is reevaluated during the iterative procedure to account for redistribution of load between the skin and stiffener. Skin strains at various locations are also compared with material allowables and the membrane strains are checked against prescribed strain limitations. Strength checks and local buckling checks are performed for the stiffener elements including the rolling mode in the case of flanged stiffeners. The torsional/flexural buckling analysis of the stiffeners takes into account the effect of the attached skin. A skin/stiffener interface stress analysis is performed as a final check at the option of the user. Design constraints relative to the skin layup may also be imposed.

The principal elements of the analyses are discussed in some detail in the following sections.

SECTION PROPERTIES AND PANEL STIFFNESSES

The geometry of the stiffener is shown in Figure 2. The width of any or all flanges may be set to zero to produce other than I-shaped cross-sections. The widths, thicknesses, and ply lay-ups of all five stiffener elements may be different. All elements are assumed to be balanced and symmetric. It is further assumed that all plate elements have a sufficient number of plies so that bending-twisting coupling in the plates may be

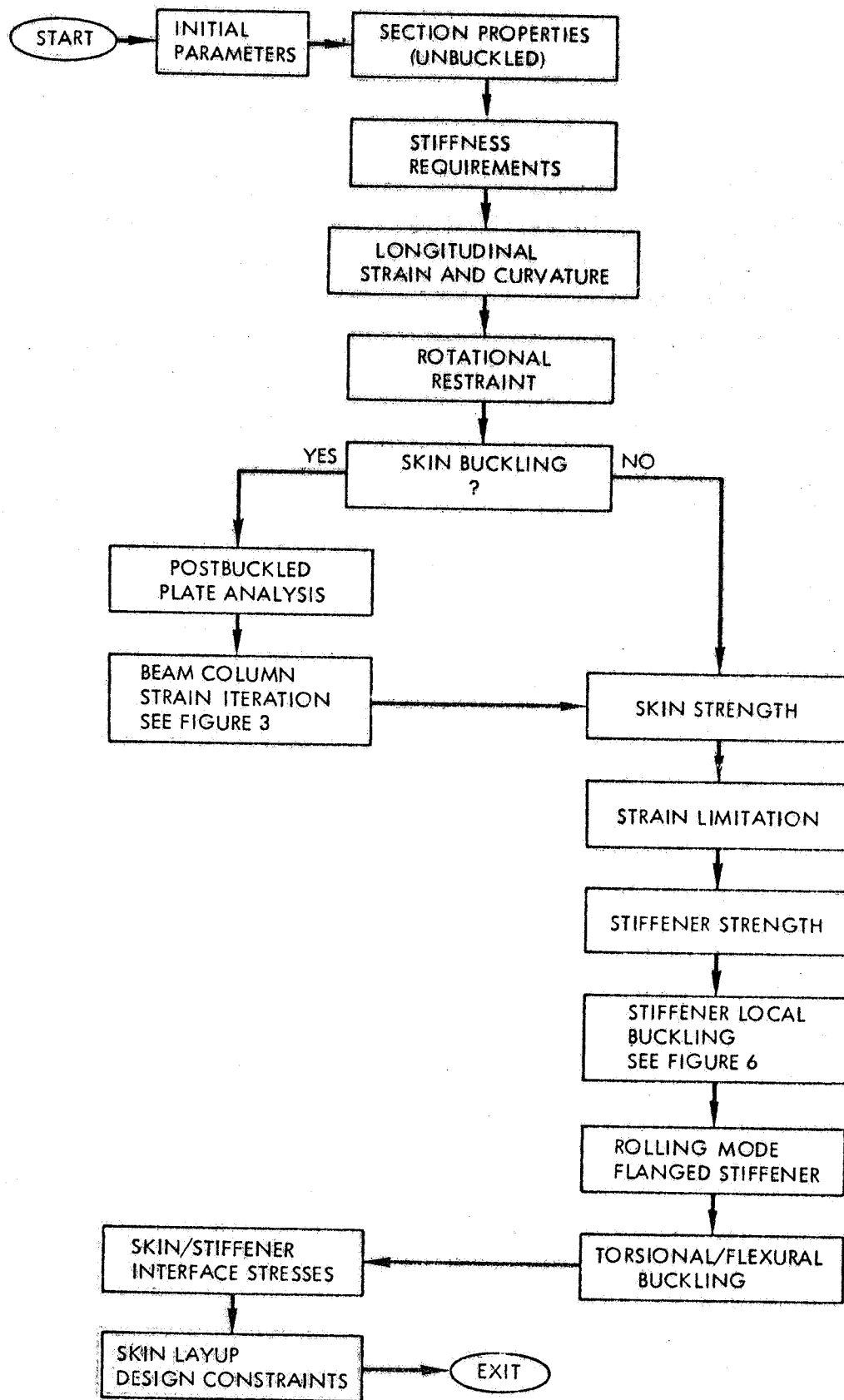


Figure 1. Flow Chart of Analysis Routines

neglected, and the plates may be treated as specially orthotropic. These requirements are normally satisfied by practical composite structures. The simplifications allowed by these assumptions greatly increase the computational efficiency of the analytical routines.

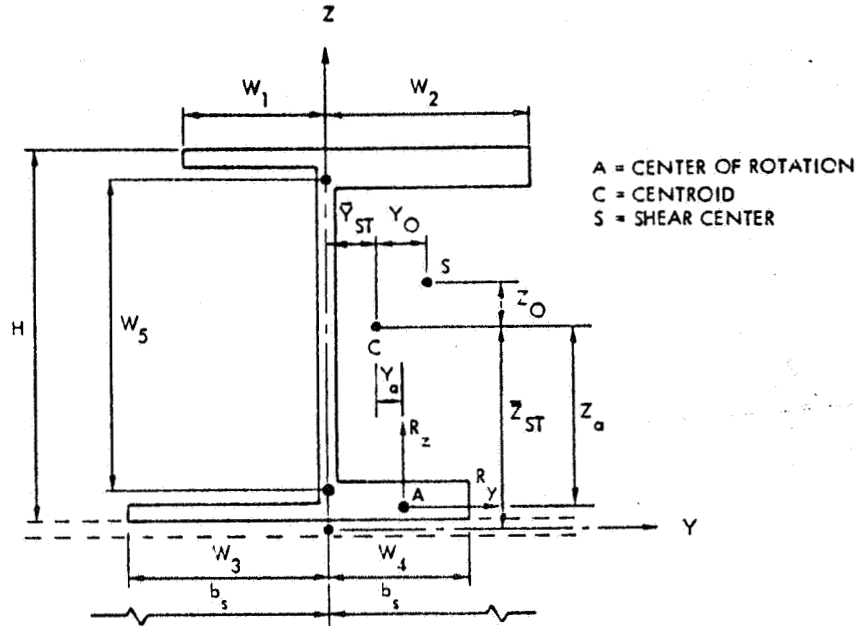


Figure 2. Stiffener Geometry

The stiffener is treated as an assemblage of plate elements in determining the extensional, bending, torsional and warping stiffnesses. Linear laminate theory is used to determine the plate inplane stiffnesses, A_{ij} , and bending stiffnesses, D_{ij} , as well as the equivalent thermal loads, N^T . The stress resultants acting in the plane of the i^{th} stiffener element are given by

$$\{N\}_i = [A]_i \{\epsilon\}_i - \{N^T\} \quad (1)$$

It is assumed that all of the N_y loading is taken by the skin. The longitudinal stress resultant in each of the stiffener elements is written in the form

$$N_{xi} = \bar{A}_{xi} \epsilon_{xi} + \nu_{x\eta i} N_{\eta i}^T - N_{xi}^T \quad (2)$$

and the longitudinal stress resultant in the skin becomes

$$N_{xsk} = \bar{A}_{xsk} \epsilon_{xsk} + \nu_{xysk} (N_y + N_{ysk}^T) - N_{xsk}^T \quad (3)$$

where the longitudinal extensional stiffness, \bar{A}_x is

$$\bar{A}_x = A_{11} - A_{12}^2/A_{22}$$

Similarly for the longitudinal bending stiffness

$$\bar{D}_x = D_{11} - D_{12}^2/D_{22}$$

The longitudinal extensional and bending stiffnesses of the panel are required in the beam-column analysis which determines the longitudinal strains and curvatures in the various elements of the panel (see Figure 2). These stiffnesses are:

$$EA_x = \sum_{i=1}^5 w_i \bar{A}_{xi} + b_s \bar{A}_{xsk} \quad (4)$$

$$EI_y = \sum_{i=1}^4 w_i \left[(\bar{A}_{xi} \bar{z}_i^2 + \bar{D}_{xi}) \right] + w_5 \bar{A}_{x5} (\bar{z}_5^2 + w_5^2/12) \\ + b_s (\bar{A}_{xsk} \bar{z}_{sk}^2 + \bar{D}_{xsk}) \quad (5)$$

where the \bar{z}_1 distances are measured from the panel centroid to the mid-surface of the plate elements. If the skin is buckled, secant or tangent values of \bar{A}_{xsk} must be used in calculating panel stiffnesses. This is discussed in more detail in the Postbuckled Plate Analysis Section.

In the torsional/flexural buckling analysis, extensional (EA), bending (EI_{yy} , EI_{yz} , EI_{zz}), torsional (GJ), and warping (C_1) stiffnesses of the stiffener are required. In calculating these stiffnesses, the portion of the skin which is integral with the attached flange of the stiffener is assumed to be part of the stiffener. Elementary beam theory is used to determine these stiffnesses as well as the location of the shear center about which the warping stiffness is computed.

BEAM-COLUMN ANALYSIS

Since the stiffnesses of the buckled skin are functions of the skin and stiffener strains and the skin strains depend on the panel stiffnesses, an iterative beam-column analysis is required to determine the strains and curvatures in the panel. If the skin is not buckled or is required to be unbuckled, only one pass through the iteration routine occurs in the analysis. Otherwise the iteration proceeds until the newly calculated longitudinal strain in the skin approximately equals the previously calculated value. A simple flow chart of the basic operations is shown in Figure 3.

After selecting any initial guess for the skin strain and calculating the stiffener properties, the unbuckled panel stiffnesses are computed. The Euler load, adjusted for stiffener shear flexibility, is defined as

$$\bar{P}_E = P_E / [1 - nP_E / (A_{66} w_5)] \quad (6)$$

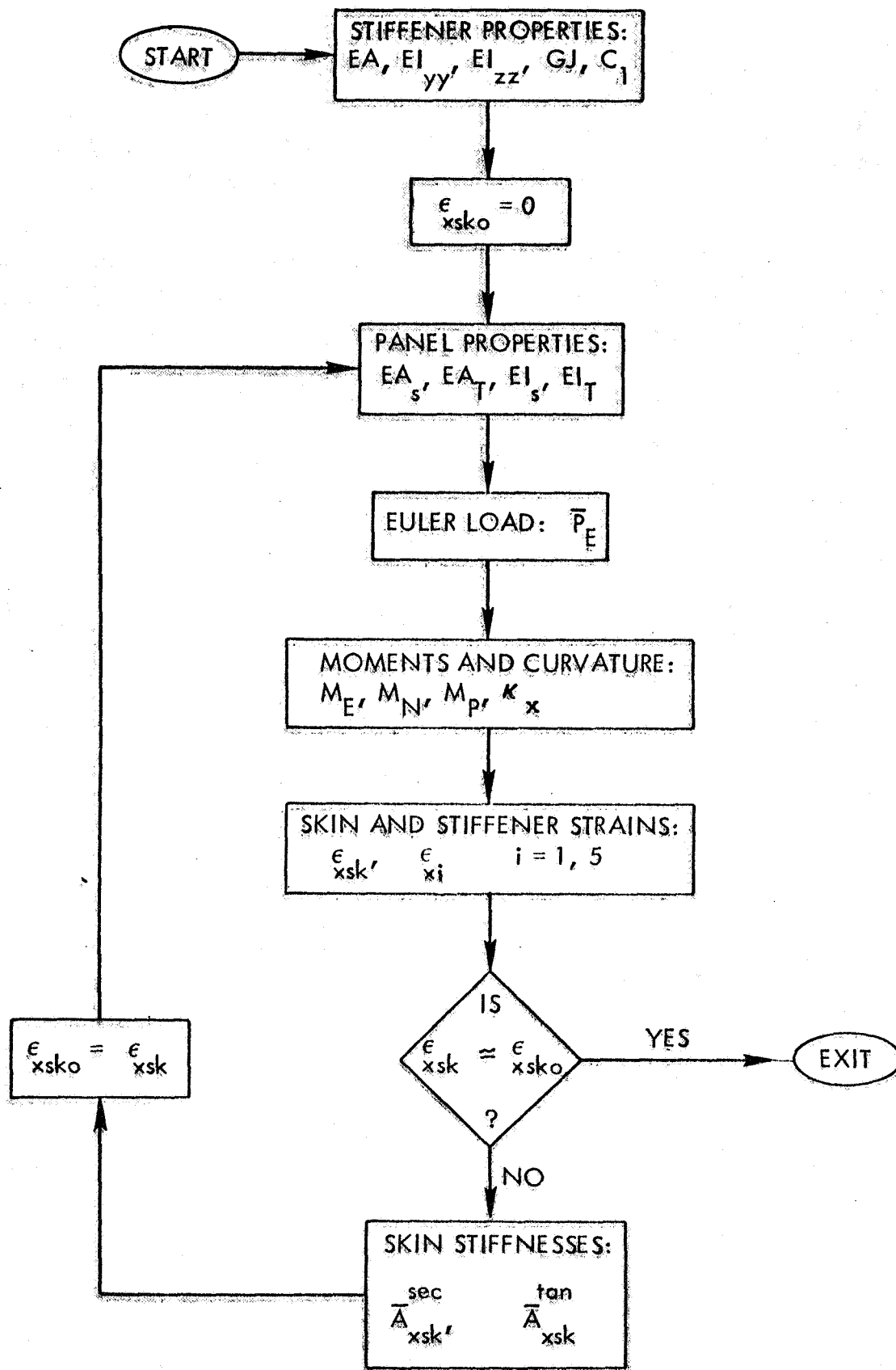


Figure 3. Flow Chart of Beam-Column Strain Iteration Routine

where A_{66} and w_5 refer to the shear stiffness and height of the web, respectively, n is the shape factor, EI_T is the tangent bending stiffness of the skin/stiffener combination, and P_E is the standard Euler load. Equation (6) is obtained from Reference 5, Section 2.17. For stiffeners having a free flange (w_1, w_2), the shape factor, n , is conservatively assumed to be 1.0. For blade stiffeners, n is taken as 1.1, a value midway between that appropriate for a rectangular cross-section (1.2) and a flanged stiffener (1.0).

The maximum moment at the panel midpoint is the sum of the moments due to initial bow, load eccentricity, and pressure

$$M = M_E + M_N + M_P \quad (7)$$

If the magnification parameters γ and μ are defined as

$$\gamma = N_x b_s / \bar{P}_E \quad (8)$$

$$\mu = \pi \sqrt{\gamma} / 2 \quad (9)$$

the moments can be written as

$$M_E = -N_x b_s e / (1 - \gamma) \quad (10)$$

$$M_N = -N_x b_s \Delta / \cos(\mu) \quad (11)$$

$$M_P = -pL^2 b_s [\sec(\mu) - 1] / 4\mu^2 \quad (12)$$

$$M_p = -pL^2 b_s [(\mu) \csc(\mu) - 1]/4\mu^2 \quad (\text{Fixed Ends}) \quad (13)$$

where

e = Initial Bow Magnitude at Midspan
(Positive Inward, Both + And - Are Checked)

Δ = Eccentricity of N_x From Centroid
(Positive Towards Skin)

p = Applied Pressure
(Positive If Internal)

The curvature at midspan is

$$\kappa_x = -M/EI_s \quad (14)$$

where EI_s is the secant bending stiffness of the panel. Although the tangent and secant stiffnesses vary along the length of the panel due to the variation of the moment along the length, the panel is conservatively assumed to have constant properties along its length based on the maximum midspan moment. If a nonzero value of "e" is specified, separate analyses are performed for +e and -e.

The longitudinal strain in any element of the panel is

$$\epsilon_{xi} = P_x/EA_s + z_i \kappa_x \quad (15)$$

in which P_x is the total equivalent longitudinal load on the panel

$$P_x = b_s [N_x - \nu_{ysk} (N_y + N_{ysk}^T) + N_{xsk}^T] + N_{ST}^T \quad (16)$$

where N_{ST}^T is the equivalent thermal load in the stiffener. Having an improved estimate of the longitudinal strain in the skin from equation (15), as well as strains in the stiffener elements, new skin secant and tangent stiffnesses can be computed. These stiffnesses are not only functions of the skin strain but also of the stiffener element strains as reflected through the stiffener rotational restraint of the skin. This rotational restraint is discussed in the following section. The iteration on skin strain continues until two consecutive values differ by less than 0.000020 inches/inch.

ROTATIONAL RESTRAINT OF SKIN

The skin plate is restrained along its long edges by the stiffener. The panel ends are assumed to be simply supported. For long wavelengths, the rotational restraint is primarily a function of the torsional stiffness of the stiffener. For short wavelengths, the web transverse bending stiffness dominates the rotational restraint. Intermediate wavelengths require interaction of the torsional stiffness of the stiffener and the bending stiffness of the web.

The torsional stiffness of the stiffener may be determined from the differential equation of a column subject to a distributed twisting moment, M_a . This equation, obtained from Section 5.5 of Reference 5, is

$$C_1 \phi_{xxxx} - (GJ - EI_O \bar{P}/EA) \phi_{xx} - \bar{P} (y_O w_{xx} - z_O v_{xx}) - R_y(z_O - z_a) + R_z(y_O - y_a) = M_a \quad (17)$$

in which EI_O is the polar bending stiffness; \bar{P} is the compression load acting on the stiffener; y_O, z_O are the shear center coordinates and y_a, z_a are the coordinates of the center of rotation relative to the centroid; and R_y and R_z are the horizontal and vertical reaction forces at the rotation center, respectively (see Figure 2).

If the skin is assumed to deform antisymmetrically about the rotation center and this point lies in the skin midplane, the vertical reaction $R_z = 0$ and $z_a = \bar{z}_{st}$ (see Figure 2). The reaction forces are given by

$$R_y = EI_{zz} v_{,xxxx}^0 + EI_{yz} w_{,xxxx}^0 + \bar{P} (v_{,xx}^0 + z_o \phi_{,xx}) \quad (18)$$

$$R_z = EI_{yz} v_{,xxxx}^0 + EI_{yy} w_{,xxxx}^0 + \bar{P} (w_{,xx}^0 - y_o \phi_{,xx}) \quad (19)$$

Assuming that the cross-section rotates without local deformation about the rotation center, as shown in Figure 4(a),

$$v_a = 0 = v^0 + (z_o - z_a) \phi \quad (20)$$

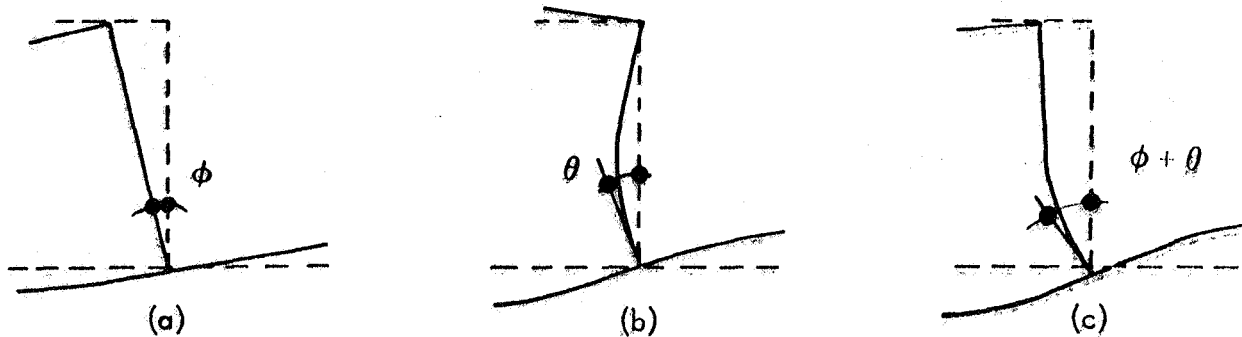


Figure 4. Stiffener Rotational Deformation

Equations (17) through (20) can be combined to yield two coupled differential equations in w and ϕ . If M_a , w , and ϕ are assumed to vary sinusoidally, the two equations may be solved to yield the torsional stiffness

$$K_{\phi} = M_a / \phi$$

$$= \frac{\pi^2}{\lambda^2} \left\{ \frac{\pi^2}{\lambda^2} [C_1 + EI_{zz} (z_o - z_a)^2] + GJ - \bar{P} (EI_o/EA - z_o^2 + z_a^2) - [EI_{yz} (z_o - z_a) \frac{\pi^2}{\lambda^2} - \bar{P} y_o]^2 / (EI_{yy} \frac{\pi^2}{\lambda^2} - \bar{P}) \right\} \quad (21)$$

where λ is the half-wavelength. As λ becomes small K_{ϕ} increases rapidly. In the limit the rotation ϕ vanishes and the stiffener deforms as shown in Figure 4(b). The rotational stiffnesses of the stiffener elements can be obtained by solving the differential equation

$$D_{11} w_{xxxxx} + 2(D_{12} + 2D_{66}) w_{xxyy} + D_{22} w_{yyyy} - N_x w_{xx} = 0 \quad (22)$$

with the appropriate boundary conditions (free or elastically restrained) at one edge and an applied sinusoidal moment at the opposite edge. The stiffness associated with this deformation is denoted

$$K_{\theta} = M_{\theta} / \theta \quad (23)$$

and is a function of wavelength, element loads and element stiffnesses. If both K_{ϕ} and K_{θ} are finite, the total deformation is as shown in Figure 4(c). The net stiffness is approximately that of two springs in series

$$K_R = 1 / (1/K_{\phi} + 1/K_{\theta}) \quad (24)$$

If the stiffener has no free flanges, cross-sectional deformation is negligible and K_R is set equal to K_{ϕ} .

POSTBUCKLED PLATE ANALYSIS

The analysis predicts the behavior of anisotropic plates loaded in the postbuckling range by a combination of in-plane biaxial compression, or tension, and shear. Derivations are based on the shear field theory developed by W. T. Koiter (Reference 6) for isotropic plates. This theory was extended to include the case of symmetrically laminated composite plates. The buckling displacement pattern used in the analysis is expressed by

$$w(x,y) = W(y) \sin \frac{\pi}{\lambda} (x-my) \quad (25)$$

in which λ is the half-wavelength of the buckle in the longitudinal (x) direction and m defines the inclination of the nodal lines in the presence of shear. To extend the analysis into the advanced postbuckling regime, the function $W(y)$ is taken as constant ($W = f$) in a center strip of width $(1 - \alpha)b_s$ and remains doubly curved in the edge zones. The buckling displacement pattern is shown in Figure 5. The Rayleigh-Ritz method is used to determine the unknown parameters, λ , m, f and α . For plates of

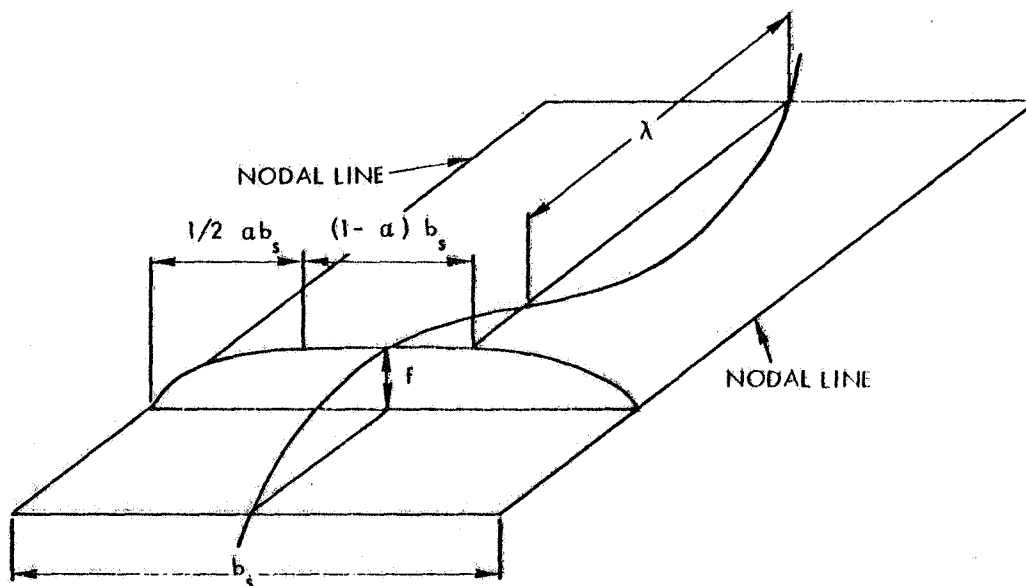


Figure 5. Post Buckling Wave Pattern

finite aspect ratio, λ must be determined so as to produce an integer number of half waves along the plate length. The correct number of half waves is that which makes the strain energy a minimum.

Average stress resultants

The total strain energy per unit surface area, including the torsional strain energy of the stiffener, may be written as

$$V = \frac{1}{2} \left\{ \frac{N_1^2}{\bar{A}_{11}} - \frac{2\nu_{xy} N_1 N_2}{\bar{A}_{11}} + \frac{N_2^2}{\bar{A}_{22}} + \frac{N_{12}^2}{A_{66}} + \frac{1}{8} F^2 [(3-2\alpha)\alpha\bar{A}_{11} D^2 + A_{22}/\alpha^3] \right. \\ \left. + \frac{1}{4} N^* F [D^2 C(2-\alpha) + \frac{1}{2} DC_2/\alpha + \mu_{22}/\alpha^3] \right\} + K_R F/(\alpha^2 b_s^2) \quad (26)$$

where

$$F = \pi^2 f^2 / (4b_s^2)$$

$$D = b_s^2 / \lambda^2$$

$$N^* = 4\pi^2 D_{11} / b_s^2$$

$$\mu_{ij} = D_{ij} / D_{11}$$

$$\mu_3 = \mu_{12} + 2\mu_{66}$$

$$C = 1 - 4\mu_{16}m + 2\mu_3 m^2 - 4\mu_{26}m^3 + \mu_{22}m^4$$

$$C_k = \partial^k C / \partial m^k \quad k = 1, 2, 3$$

The rotational restraint (K_R) is a function of λ and of the stiffener load (see Rotational Restraint of Skin). The average stress resultants, N_1 , N_2 , and N_{12} acting on the postbuckled panel may be written in terms of the panel edge strain, ϵ_1 , ϵ_2 , and γ_{12} , and the wave shape parameters D , F , m , and α .

$$\begin{aligned} N_1 &= A_{11} \epsilon_1 + A_{12} \epsilon_2 + (A_{11} + A_{12} m^2) (1 - \alpha/2) DF + A_{12} F/(2\alpha) \\ N_2 &= A_{12} \epsilon_1 + A_{22} \epsilon_2 + (A_{12} + A_{22} m^2) (1 - \alpha/2) DF + A_{22} F/(2\alpha) \quad (27) \\ N_{12} &= A_{66} [\gamma_{12} - (2-\alpha)mDF] \end{aligned}$$

Differentiating the strain energy equation (26), with respect to F , m , and α , for a given value of D , yields three equations from which these three parameters can be determined.

$$\begin{aligned} N_1 D(2-\alpha) + N_2 [m^2 D(2-\alpha) + 1/\alpha] - 2N_{12} mD(2-\alpha) + 2K_R/(\alpha^2 b_s) + \\ \frac{1}{4} F [(3-2\alpha) \alpha \bar{A}_{11} D^2 + A_{22}/\alpha^3] + \frac{1}{4} N^* [D^2 C(2-\alpha) + \frac{1}{2} DC_2/\alpha + \mu_{22}/\alpha^3] = 0 \quad (28) \end{aligned}$$

$$N_2 m(2-\alpha) - N_{12} (2-\alpha) + \frac{1}{8} N^* [DC_1(2-\alpha) + \frac{1}{2} C_3/\alpha] = 0 \quad (29)$$

$$\begin{aligned} N_1 D + N_2 (m^2 D + 1/\alpha^2) - 2N_{12} mD - \frac{1}{8} F [(3-4\alpha) \bar{A}_{11} D^2 - 3A_{22}/\alpha^4] \\ + \frac{1}{4} N^* [D^2 C + \frac{1}{2} DC_2/\alpha^2 + 3\mu_{22}/\alpha^4] + 4K_R/(\alpha^3 b_s) = 0 \quad (30) \end{aligned}$$

Since equation (30) was obtained by differentiation with respect to α , it is not valid in the initial postbuckling region where α maintains a value of 1.0 over a range of loads greater than the initial buckling load.

Initial buckling of skin

At the onset of buckling $\alpha = 1$ and $F = 0$. Equations (28) and (29) may then be written

$$N_1 D + N_2 (m^2 D + 1) - 2N_{12} m D + \frac{1}{4} N^* (D^2 C + \frac{1}{2} D C_2 + \mu_{22}) + \frac{2}{b_s} K_R = 0 \quad (31)$$

$$N_2 m - N_{12} + \frac{1}{8} N^* (D C_1 + \frac{1}{2} C_3) = 0 \quad (32)$$

For specified values of N_2 and N_{12} , the quantity m can be determined from equation (32) by iteration, for a given value of D (wavelength). The above parameters together with a preliminary value of K_R may be substituted in equation (31) to yield the corresponding load N_1 . Since K_R is a function of stiffener load as well as wavelength, the correct value of N_1 again must be found by iteration.

The average stress resultant N_1 is calculated for a series of wavelengths. The minimum value of N_1 corresponds to the initial buckling load N_{1CR} .

Strains in buckled skin

As one of the failure modes considered in the analysis, strains, or stresses, in the skin are compared with material allowables. The maximum longitudinal membrane strain (ϵ_1) in the skin occurs along the nodal lines parallel to the stiffener. This strain increases with increasing load. The longitudinal membrane strain in the center portion of the skin between two stiffeners on the other hand, remains essentially constant and equal to its value at initial buckling. Large bending strains exist in this region of the skin and, as a result, the total compressive strain in the center portion of the skin may exceed the strain in the skin at the stiffener

location. In the center region of the skin, the middle surface strains are given by

$$\begin{aligned}\epsilon_x &= \epsilon_1 + FD \\ \epsilon_y &= \epsilon_2 + FD [m^2(1-\alpha/2) - \nu_{xy} \alpha/2] + F/(2\alpha) \\ \gamma_{xy} &= \gamma_{12} - 2FDm(1 - \alpha/2)\end{aligned}\tag{33}$$

The curvatures in the center portion of the skin vary sinusoidally in the longitudinal direction

$$\begin{aligned}w_{,xx} &= -2\pi DF^{1/2}/b_s \sin \pi(x-my)/L \\ w_{,yy} &= m^2 w_{,xx} \\ w_{,xy} &= -mw_{,xx}\end{aligned}\tag{34}$$

The strains in each ply are computed at the four potentially critical points defined by $(x,y)=(0,0)$, $(\lambda/2, 0)$, $(0, b_s/2)$, and $(\lambda/2, b_s/2)$. The skin strength margin of safety corresponds to the ply and the location where the lowest margin of safety exists according to the maximum strain criterion or the Tsai-Hill criterion.

Buckled skin stiffnesses

For stability calculations, the stiffness matrix of the buckled skin with respect to incremental deformations must be known. In terms of the average stress resultants in the skin, N_1 , N_2 and $N_6 = N_{12}$, and the strains in the skin at the stiffener locations, ϵ_1 , ϵ_2 and $\epsilon_6 = \gamma_{12}$, the incremental load-strain relationships may be written as:

$$\begin{Bmatrix} dN_1 \\ dN_2 \\ dN_{12} \end{Bmatrix} = \begin{bmatrix} a_{11} & a_{12} & a_{16} \\ a_{12} & a_{22} & a_{26} \\ a_{16} & a_{26} & a_{66} \end{bmatrix} \begin{Bmatrix} d\epsilon_1 \\ d\epsilon_2 \\ d\gamma_{12} \end{Bmatrix}\tag{35}$$

so that the coefficients of the tangent stiffness matrix are given by

$$a_{ij} = \frac{\partial N_i}{\partial \epsilon_j} \quad i, j = 1, 2, 6 \quad (36)$$

To determine the coefficients a_{ij} , equations (27) are differentiated with respect to ϵ_j . This yields equations in the form

$$\begin{Bmatrix} a_{j1} \\ a_{j2} \\ a_{j6} \end{Bmatrix} = \begin{bmatrix} b_{11} & b_{12} & b_{13} \\ b_{21} & b_{22} & b_{23} \\ b_{31} & b_{32} & b_{33} \end{bmatrix} \begin{Bmatrix} F_j \\ m_j \\ \alpha_j \end{Bmatrix} + \begin{Bmatrix} B_1 \\ B_2 \\ B_3 \end{Bmatrix}_j \quad j=1,2,6 \quad (37)$$

where

$$\begin{Bmatrix} F_j \\ m_j \\ \alpha_j \end{Bmatrix} = \frac{\partial}{\partial \epsilon_j} \begin{Bmatrix} F \\ m \\ \alpha \end{Bmatrix}$$

Differentiating equations (28) through (30) with respect to ϵ_j gives

$$\begin{bmatrix} c_{11} & c_{12} & c_{13} \\ c_{21} & c_{22} & c_{23} \\ c_{31} & c_{32} & c_{33} \end{bmatrix} \begin{Bmatrix} a_{j1} \\ a_{j2} \\ a_{j6} \end{Bmatrix} + \begin{bmatrix} d_{11} & d_{12} & d_{13} \\ d_{21} & d_{22} & d_{23} \\ d_{31} & d_{32} & d_{33} \end{bmatrix} \begin{Bmatrix} F_j \\ m_j \\ \alpha_j \end{Bmatrix} = 0 \quad (38)$$

$$j = 1, 2, 6$$

Simultaneous solution of equations (37) and (38) yields the tangent stiffness coefficients a_{ij} .

Longitudinal tangent and secant stiffnesses of the buckled skin are required to calculate section properties for use in the beam column analysis. The longitudinal tangent stiffness

$$\bar{A}_{xsk} \tan = \frac{dN_1}{d\epsilon_1}$$

is determined as follows. Inversion of equation (35) yields

$$\{d\epsilon\} = [a^*] dN$$

Since the average stress resultants N_1 and N_{12} are assumed constant in the postbuckling regime, $dN_2 = dN_{12} = 0$ and hence

$$\bar{A}_{xsk} \tan = \frac{dN_1}{d\epsilon_1} = \frac{1}{a_{11}^*} \quad (39)$$

The longitudinal secant stiffness is given by

$$\bar{A}_{xsk}^{sec} = \frac{N_1 + N_{xsk}^T - \nu_{xysk} (N_y + N_{ysk}^T)}{\epsilon_1 + [N_{xsk}^T - \nu_{xysk} N_{ysk}^T] / \bar{A}_{11}} \quad (40)$$

DESIGN STRAIN LIMITATIONS

Structures currently designed with composite materials are limited to design ultimate strain levels substantially below the failure strains of the basic composite material. The two principal factors establishing these limits are (1) stress concentrations associated with cutouts, joints and splices for structures loaded in tension, and (2) tolerance for impact damage for compression critical structures. Other considerations are: transverse cracking in plies perpendicular to the major loading direction, temperature and humidity, compatibility with adjacent metallic structures, manufacturing defects, and repairability.

In POSTOP, tension and compression strain limitations in the fiber direction and transverse direction may be specified by the user. These limitations are applied at the ply level to the skin membrane strains only.

Local bending strains due to pressure loading and postbuckling are not included in checks against these limitations. Likewise thermal strains are excluded. Membrane strains in the skin resulting from panel bending due to eccentricities, pressure, and skin buckling, however, are included and added to those caused by in-plane loading.

STIFFENER STRENGTH

The strength of the stiffener is based on the maximum strain criterion or the Tsai-Hill criterion as applied to the critical element of the stiffener. This element is the free flange, if one is present, or the free edge of a blade stiffener. Longitudinal strain, ϵ_{xi} , is computed from equation (15). Since the transverse applied load and in-plane shear are zero, the transverse and shear strains are

$$\epsilon_{yi} = (-A_{12} \epsilon_{xi} + N_{yi}^T) / A_{22}$$

$$\gamma_{xyi} = 0$$

where N_{yi}^T is the transverse thermal load in the element. If the stiffener is a blade, the curvatures of the web about its midplane are set equal to zero. If a free flange is present, the longitudinal curvature about its midplane is set equal to the panel curvature as given by equation (14). All other curvatures are set equal to zero. Strains are calculated at each ply and the critical margin of safety is computed according to the specified criterion.

Local bending and twisting strains in the stiffener elements due to postbuckling deformations in the skin are currently neglected in the analysis.

STIFFENER LOCAL BUCKLING

The skin is allowed to buckle locally in POSTOP as discussed previously. The wavelength at initial buckling is $2\lambda_{ib}$. As the skin is loaded further into the postbuckling range, the critical wavelength decreases. POSTOP requires the stiffener to offer positive rotational restraint to the skin in all wavelengths shorter than $2\lambda_{ib}$.

The stiffener will therefore always restrain the skin and will not tend to drive the skin or to force it to have a stiffener dominated wavelength. For the longer wavelengths ($\lambda > \lambda_{ib}$), it is assumed that the stiffener may be restrained against local buckling by the skin. For panels with normal geometry, this restraint will be advantageous only in the case of panels with blade stiffeners. The critical wavelength for local buckling of flanged stiffeners is normally smaller than the critical skin buckling wavelength ($\lambda < \lambda_{ib}$). Torsional/flexural buckling will govern at the longer wavelengths. The local buckling analysis is performed for all half-wavelengths from $\lambda = L$ to $\lambda_N = L/N_{max}$, where N_{max} is a user defined maximum number of wavelengths. For $\lambda_N > \lambda_{ib}$ the skin rotational stiffness, K_{sk} , is conservatively estimated as $4D_{22}/b_s$. Here D_{22} is the skin transverse bending stiffness neglecting the additional stiffness due to the attached flange. In panels with buckled skin, the out-of-plane deformations of the skin increase the transverse bending stiffness over that of a flat, unbuckled plate for $\lambda_N > \lambda_{ib}$. The conservatism in the estimated rotational stiffness, $4D_{22}/b_s$, may therefore be extreme for highly postbuckled panels. A summary of the stiffener local buckling calculations is shown in the flow chart in Figure 6.

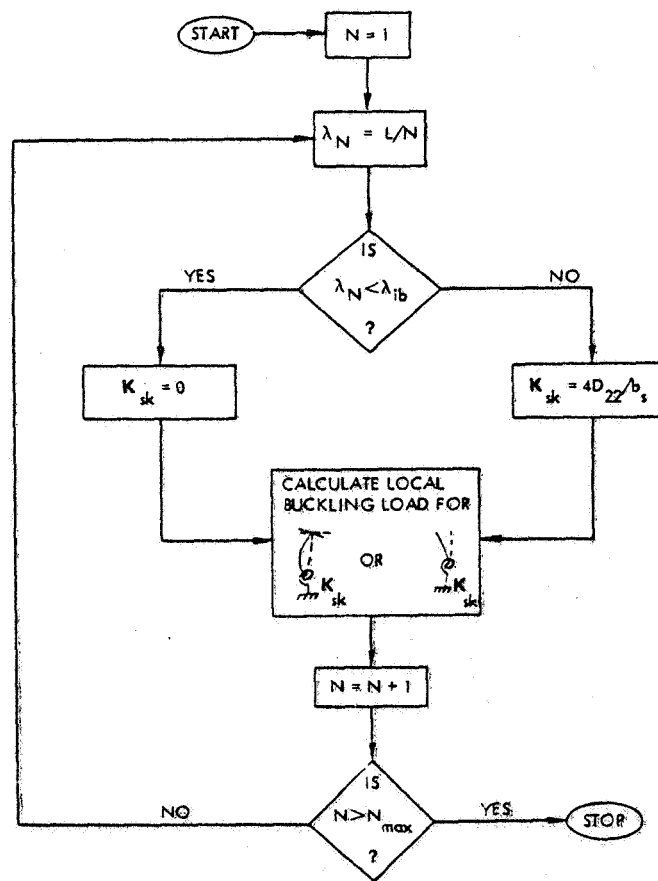


Figure 6. Flow Chart of Stiffener Local Buckling Analysis

The local buckling analysis of the stiffener for a given wavelength assumes that each stiffener element is uniformly loaded in pure compression. This assumption is approximated in the stiffener web of a panel loaded in bending due to eccentricities or pressure by taking the load at the web midheight as the magnitude of the uniform load. Figure 4(b) shows the deformation associated with stiffener local buckling.

The rotational stiffnesses of the stiffener elements are obtained from the solution to equation (22). First the free flange rotational stiffnesses are obtained from the solution for a plate with one edge free and a sinusoidal moment applied at the opposite edge. The stiffener web/skin junction rotational stiffness, K_θ as defined in equation (23), is then obtained from the solution for a plate restrained by the flange rotational stiffness at the far edge and subject to a sinusoidal moment at the near edge. The factor by which the actual element loads must be multiplied to give neutral stability is found by iteration for each wavelength. Neutral stability corresponds to $K_\theta + K_{sk} = 0$. The margin of safety is equal to the lowest load factor minus one.

ROLLING OF STIFFENERS

While stiffener stability at short wavelengths is governed by local buckling, torsional modes become critical at long wavelengths. If the skin is very flexible in bending, as is normally the case in buckled panels, the critical long wave modes will be torsional/flexural with essentially rigid cross-sectional rotation. This mode is discussed in the following section. If the skin is very rigid in bending, a torsional mode, as shown in Figure 7 for a rigid skin, could be critical at long wavelengths. This will be referred to as the rolling mode. In lieu of a more accurate, coupled torsional analysis combining both the rolling and torsional/flexural modes, two simpler analyses are used in POSTOP.

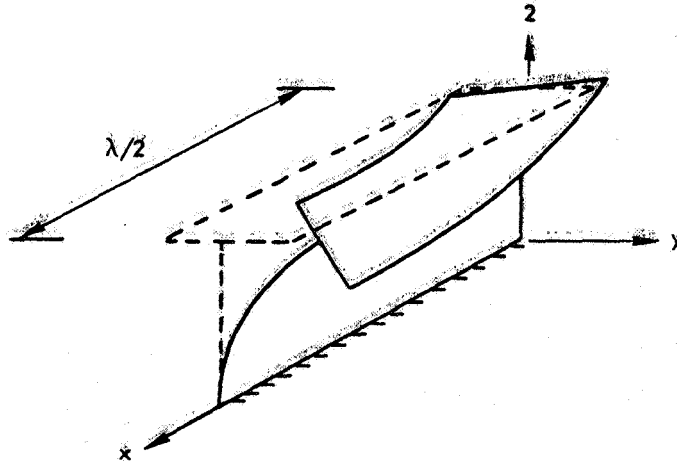


Figure 7. Rolling Deformation

Using an assumed displacement field for the stiffener deformation in the rolling mode, the total potential energy may be expressed and minimized to determine the critical load factor. Here the displacement field assumed is (Reference 7)

$$\begin{aligned} u &= -Cz^2 y \frac{\pi}{\lambda} \cos \frac{\pi}{\lambda} x \\ v &= Cz^2 \sin \frac{\pi}{\lambda} x \\ w &= -2Czy \sin \frac{\pi}{\lambda} x \end{aligned} \quad (41)$$

in which u , v , and w are the displacements in the x , y , and z coordinate directions shown in Figure 7.

Neglecting bending energy terms in the flange compared to the membrane terms, the load factor, R , for stiffener rolling in a given wavelength can be written as

$$\begin{aligned} R = & \left\{ \left[\left(\frac{\pi}{\lambda} \right)^2 D_{11} w_5^4/5 - 4w_5^2 D_{12}/3 + 4D_{22}/\left(\frac{\pi}{\lambda} \right)^2 + 16w_5^2 D_{66}/3 \right]_{web} \right. \\ & \left. + \left(\frac{\pi}{\lambda} \right)^2 w_5^3 [\bar{A}_{x1} w_1^3 + \bar{A}_{x2} w_2^3] \right\} / w_5^3 [N_{x5} w_5/5 + N_{x1} w_1 + N_{x2} w_2] \end{aligned} \quad (42)$$

The lowest value of the load factor is found for wavelengths ranging from the panel length to the stiffener spacing. The margin of safety is equal to the lowest load factor minus one:

TORSIONAL/FLEXURAL BUCKLING OF STIFFENERS

In the analysis it is assumed that the stiffeners are cocured or bonded to the skin and the portion of the skin that is integral with the stiffener flange is considered part of the stiffener. The remaining skin on each side of the stiffener is assumed to be detached and replaced by a set of equivalent stress resultants. These stress resultants (and couples) are considered to act as external loads on the stiffener, as shown in Figure 8. The buckling mode is assumed to be periodic along the width direction with one period 'p' including one or more stringers (see Figure 9).

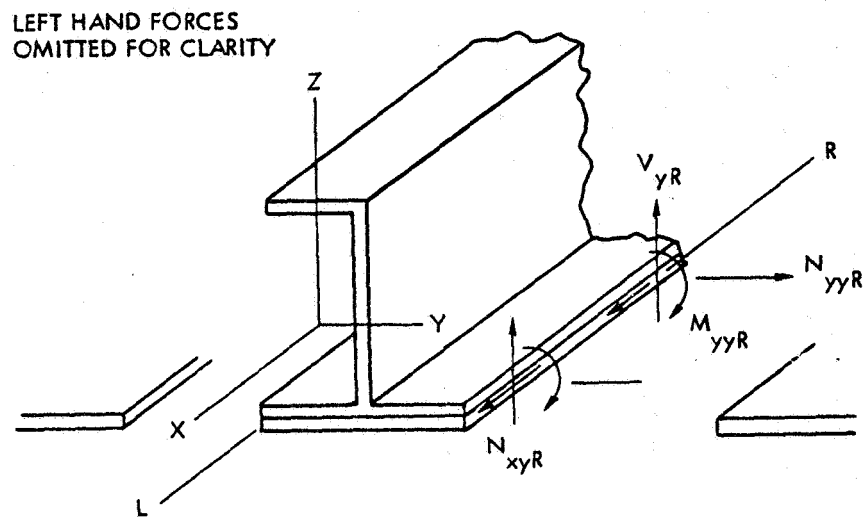


Figure 8. Skin Forces Acting on Stiffener

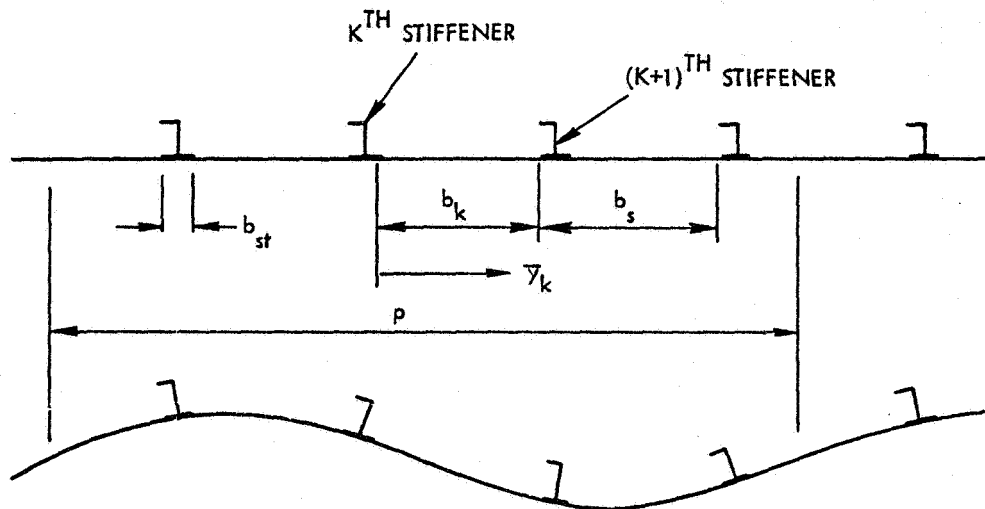


Figure 9. Transverse Mode Shape

In determining the constraint forces, membrane and flexural effects are assumed to be uncoupled and treated independently. A section of skin between the k^{th} and $(k+1)^{th}$ stiffener of width $b_k = b_s - b_{st}$ is analyzed.

Calculation of membrane forces acting on stiffener

If $\bar{u}^{(k)}$ and $\bar{v}^{(k)}$ represent the displacements of the skin in the \bar{x} and \bar{y} directions measured with respect to the prebuckling configuration, inplane equilibrium yields the following two governing differential equations.

$$\begin{aligned} A_{11} \bar{u}_{,xx}^{(k)} + A_{66} \bar{u}_{,yy}^{(k)} + (A_{12} + A_{66}) \bar{v}_{,xy}^{(k)} &= 0 \\ (A_{12} + A_{66}) \bar{u}_{,xy}^{(k)} + A_{66} \bar{v}_{,xx}^{(k)} + A_{22} \bar{v}_{,yy}^{(k)} &= 0 \end{aligned} \quad (43)$$

By letting

$$\begin{aligned} \bar{u}^{(k)} &= U^{(k)}(\bar{y}) \cos \bar{n}x \\ \bar{v}^{(k)} &= V^{(k)}(\bar{y}) \sin \bar{n}x \end{aligned} \quad (44)$$

in which $\bar{n} = n\pi/L$, and substituting equation (44) into equation (43), the following uncoupled fourth order differential equation in $U^{(k)}$ is obtained.

$$U^{iv(k)} - \bar{n}^2 (A_{11}/A_{66} - 2A_{12}/A_{22}) U^{ii(k)} + \bar{n}^4 (A_{11}/A_{22}) U^{(k)} = 0 \quad (45)$$

The solution to equation (45) can be put in the form

$$U^{(k)} = \sum_{j=1}^4 A_j^{(k)} f_j(\bar{y}) \quad (46)$$

where f_j are known functions of \bar{y} and $A_j^{(k)}$ are constants of integration. Substituting equation (46) into the first of equations (43) and integrating yields an expression for $V^{(k)}$ which may be written in the form

$$V^{(k)} = \sum_{j=1}^4 A_j^{(k)} g_j(\bar{y}) \quad (47)$$

The integration constants may be expressed in terms of the buckling displacements of the k^{th} and $(k+1)^{\text{th}}$ stiffeners by imposing conditions of continuity between skin and stringers at the left (L) and right (R) attachment lines shown in Figure 8. Denoting the longitudinal displacement of the stiffener during buckling by u^0 , the displacements of the shear center in the y and z directions by v^0 and w^0 , respectively, and the twist per unit length by ϕ , the displacements of the stringer at an arbitrary point q of the cross-section may be expressed as

$$\begin{aligned} u_q &= u^0 - y_q v_{,x}^0 - z_q w_{,x}^0 + (\bar{\omega}_s - \omega_q) \phi, \\ v_q &= v^0 - (z_q - z_0) \phi \\ w_q &= w^0 + (y_q - y_0) \phi \end{aligned} \quad (48)$$

The coordinates of the shear center (y_0, z_0) and those of point q (y_q, z_q) are measured with respect to the centroid. The last term in the first of equations (48) represent the displacement due to warping of the cross-section at q . To satisfy inplane continuity between skin and stiffeners at the attachment lines, the following conditions are prescribed.

$$\begin{aligned} u_R^{(k)} &= \bar{u}^{(k)} \left(\begin{array}{c} \bar{x}=x \\ \bar{y}=0 \end{array} \right) & v_R^{(k)} &= \bar{v}^{(k)} \left(\begin{array}{c} \bar{x}=x \\ \bar{y}=0 \end{array} \right) \\ u_L^{(k+1)} &= \bar{u}^{(k)} \left(\begin{array}{c} \bar{x}=x \\ \bar{y}=b_k \end{array} \right) & v_L^{(k+1)} &= \bar{v}^{(k)} \left(\begin{array}{c} \bar{x}=x \\ \bar{y}=b_k \end{array} \right) \end{aligned} \quad (49)$$

By substituting equations (46) and (47) into equations (44) and using the results together with equation (48) in the boundary conditions (49), one may solve for the integration constants in the form

$$\begin{Bmatrix} A_1 \\ A_2 \\ A_3 \\ A_4 \end{Bmatrix}^{(k)} \cos \bar{n}x = [R] \begin{Bmatrix} u^0 \\ v_{,x}^0 \\ w_{,x}^0 \\ \phi_{,x} \end{Bmatrix}^{(k)} + [L] \begin{Bmatrix} u^0 \\ v_{,x}^0 \\ w_{,x}^0 \\ \phi_{,x} \end{Bmatrix}^{(k+1)} \quad (50)$$

where the terms in the 4×4 matrices $[R]$ and $[L]$ are functions of $f_j(\bar{y})$ and $g_j(\bar{y})$ at $\bar{y} = 0$ and $\bar{y} = b_k$, respectively.

If there are N stiffeners within one period, there will be N equations of this type. The N^{th} equations, however, becomes

$$\begin{Bmatrix} A_1 \\ A_2 \\ A_3 \\ A_4 \end{Bmatrix}^{(N)} \cos \bar{n}x = [R] \begin{Bmatrix} u^0 \\ v_{,x}^0 \\ w_{,x}^0 \\ \phi_{,x} \end{Bmatrix}^{(N)} + [L] \begin{Bmatrix} u^0 \\ v_{,x}^0 \\ w_{,x}^0 \\ \phi_{,x} \end{Bmatrix}^{(1)} \quad (51)$$

The constraint forces $N_{yy}^{(k)}$ and $N_{xy}^{(k)}$ acting on the k^{th} stringer may now be determined in terms of the displacements and twist of that stringer and the adjacent ones, or

$$\begin{aligned} N_{yyR}^{(k)} &= S_{R1} u_{,x}^{(k)} + S_{R2} v_{,xx}^{(k)} + S_{R3} w_{,xx}^{(k)} + S_{R4} \phi_{,xx}^{(k)} \\ &\quad + S_{L1} u_{,x}^{(k+1)} + S_{L2} v_{,xx}^{(k+1)} + S_{L3} w_{,xx}^{(k+1)} + S_{L4} \phi_{,xx}^{(k+1)} \\ N_{yyL}^{(k)} &= \bar{S}_{R1} u_{,x}^{(k-1)} + \bar{S}_{R2} v_{,xx}^{(k-1)} + \bar{S}_{R3} w_{,xx}^{(k-1)} + \bar{S}_{R4} \phi_{,xx}^{(k-1)} \\ &\quad + \bar{S}_{L1} u_{,x}^{(k)} + \bar{S}_{L2} v_{,xx}^{(k)} + \bar{S}_{L3} w_{,xx}^{(k)} + \bar{S}_{L4} \phi_{,xx}^{(k)} \end{aligned}$$

$$\begin{aligned}
N_{xyR}^{(k)} &= T_{R_1} u^{(k)} + T_{R_2} v_{,x}^{(k)} + T_{R_3} w_{,x}^{(k)} + T_{R_4} \phi_{,x}^{(k)} \\
&\quad + T_{L_1} u^{(k+1)} + T_{L_2} v_{,x}^{(k+1)} + T_{L_3} w_{,x}^{(k+1)} + T_{L_4} \phi_{,x}^{(k+1)} \quad (52) \\
N_{xyL}^{(k)} &= \bar{T}_{R_1} u^{(k-1)} + \bar{T}_{R_2} v_{,x}^{(k-1)} + \bar{T}_{R_3} w_{,x}^{(k-1)} + \bar{T}_{R_4} \phi_{,x}^{(k-1)} \\
&\quad + \bar{T}_{L_1} u^{(k)} + \bar{T}_{L_2} v_{,x}^{(k)} + \bar{T}_{L_3} w_{,x}^{(k)} + \bar{T}_{L_4} \phi_{,x}^{(k)}
\end{aligned}$$

where the terms S_{R_j} , \bar{S}_{R_j} , T_{R_j} , and \bar{T}_{R_j} are functions of the matrix coefficients R_{ij} . The terms S_{L_j} , \bar{S}_{L_j} , T_{L_j} , \bar{T}_{L_j} are functions of the matrix coefficients L_{ij} .

Effect of skin bending on stiffener buckling

The governing differential equation for plate bending in the presence of membrane forces (\bar{N}_{xx} , \bar{N}_{yy} , \bar{N}_{xy}) may be written

$$\begin{aligned}
D_{11} \bar{w}_{,xxxx}^{(k)} + 4D_{16} \bar{w}_{,xxxxy}^{(k)} + 2(D_{12} + 2D_{66}) \bar{w}_{,xxxyy}^{(k)} + 4D_{26} \bar{w}_{,xyyy}^{(k)} \\
+ D_{22} \bar{w}_{,yyyy}^{(k)} - \bar{N}_{xx} \bar{w}_{,xx}^{(k)} - 2\bar{N}_{xy} \bar{w}_{,xy}^{(k)} - \bar{N}_{yy} \bar{w}_{,yy}^{(k)} - p^{(k)} = 0
\end{aligned}$$

where \bar{w} is the normal displacement of the skin panel with respect to the pre-buckling configuration and p is the normal pressure.

In determining the flexural effects of the attached skin, the stress resultants \bar{N}_{xx} and \bar{N}_{yy} are treated as constant loads. In order to simplify the analysis, membrane shear \bar{N}_{xy} is not included and the bending-twisting stiffness terms D_{16} and D_{26} are assumed to be zero. In the absence of normal loading, the governing differential equation reduces to

$$D_{11} \bar{w}_{,xxxx}^{(k)} + 2D_3 \bar{w}_{,xxxyy}^{(k)} + D_{22} \bar{w}_{,yyyy}^{(k)} - \bar{N}_{xx} \bar{w}_{,xx}^{(k)} - \bar{N}_{yy} \bar{w}_{,yy}^{(k)} = 0 \quad (53)$$

where

$$D_3 = D_{12} + 2D_{66}$$

Representing the normal displacement as

$$\bar{w}^{(k)} = W^{(k)}(\bar{y}) \sin \bar{n}x \quad (54)$$

and defining

$$g = [D_3 + \bar{N}_{YY}/(2\bar{n}^2)]/D_{22}$$

$$1 - \bar{\mu}^2 = (D_{11} + \bar{N}_{XX}/\bar{n}^2)/(D_{22}g^2)$$

equation (53) may be written in the following form.

$$W^{iv(k)} - 2g\bar{n}^2 W^{ii(k)} + g^2(1 - \bar{\mu}^2)\bar{n}^4 W^{(k)} = 0 \quad (55)$$

The solution of the differential equation (55) depends on the values $\bar{\mu}^2$ and g . The general form of the solution may be written as

$$W^{(k)} = \sum_{j=1}^4 C_j^{(k)} F_j(\bar{y}) \quad (56)$$

The integration constants $C_j^{(k)}$ are solved in terms of the buckling displacements of the k^{th} and $(k+1)^{th}$ stiffeners by requiring the following conditions to be satisfied

$$\begin{aligned} w_R^{(k)} &= \bar{w}^{(k)} \left(\begin{matrix} \bar{x}=x \\ \bar{y}=0 \end{matrix} \right) & \phi_R^{(k)} &= \bar{w}'^{(k)}_y \left(\begin{matrix} \bar{x}=x \\ \bar{y}=0 \end{matrix} \right) \\ w_L^{(k+1)} &= \bar{w}^{(k)} \left(\begin{matrix} \bar{x}=x \\ \bar{y}=b_k \end{matrix} \right) & \phi_L^{(k+1)} &= \bar{w}'^{(k)}_y \left(\begin{matrix} \bar{x}=x \\ \bar{y}=b_k \end{matrix} \right) \end{aligned} \quad (57)$$

Using the third of equations (48) in conjunction with equations (54) and (56) one obtains the solution for the integration constants of the k^{th} stiffener in the form

$$\begin{Bmatrix} C_1 \\ C_2 \\ C_3 \\ C_4 \end{Bmatrix}^{(k)} \sin \bar{n}x = [\bar{R}] \begin{Bmatrix} w^o \\ \phi \end{Bmatrix}^{(k)} + [\bar{L}] \begin{Bmatrix} w^o \\ \phi \end{Bmatrix}^{(k+1)} \quad (58)$$

where the terms in the 4×4 matrices $[\bar{R}]$ and $[\bar{L}]$ are functions of the $F_j(\bar{y})$. For the N^{th} stiffener

$$\begin{Bmatrix} C_1 \\ C_2 \\ C_3 \\ C_4 \end{Bmatrix}^{(N)} \sin \bar{n}x = [\bar{R}] \begin{Bmatrix} w^o \\ \phi \end{Bmatrix}^{(N)} + [\bar{L}] \begin{Bmatrix} w^o \\ \phi \end{Bmatrix}^{(1)} \quad (59)$$

The moments and shear forces acting on the k^{th} stiffener can now be obtained in terms of the normal displacements and twists of the k^{th} stiffener and the adjacent stiffeners.

$$\begin{aligned} M_{YYR}^{(k)} &= B_{R1} w_o^{(k)} + B_{R2} \phi^{(k)} + B_{L1} w_o^{(k+1)} + B_{L2} \phi^{(k+1)} \\ M_{YYL}^{(k)} &= \bar{B}_{R1} w_o^{(k-1)} + \bar{B}_{R2} \phi^{(k-1)} + \bar{B}_{L1} w_o^{(k)} + \bar{B}_{L2} \phi^{(k)} \\ V_{YR}^{(k)} &= R_{R1} w_o^{(k)} + R_{R2} \phi^{(k)} + R_{L1} w_o^{(k+1)} + R_{L2} \phi^{(k+1)} \\ V_{YL}^{(k)} &= \bar{R}_{R1} w_o^{(k-1)} + \bar{R}_{R2} \phi^{(k-1)} + \bar{R}_{L1} w_o^{(k)} + \bar{R}_{L2} \phi^{(k)} \end{aligned} \quad (60)$$

The terms B_{Rj} , \bar{B}_{Rj} , R_{Rj} , and \bar{R}_{Rj} are functions of the matrix coefficients R_{ij} . The terms B_{Lj} , \bar{B}_{Lj} , R_{Lj} , and \bar{R}_{Lj} are functions of the matrix coefficients L_{ij} .

Formulation of stability matrix

Differential equations are obtained by considering equilibrium of forces and moments acting on a small element of the stiffener. Included in these forces and moments are those applied along the left (L) and right (R) attachment lines by the skin during buckling.

The moments, M_y and M_z , and the torque M_x , may be expressed in terms of the stiffener displacements and twist

$$\begin{aligned} M_y &= -EI_{yz} v_{,xx}^0 - EI_{yy} w_{,xx}^0 \\ M_z &= -EI_{zz} v_{,xx}^0 - EI_{yz} w_{,xx}^0 \end{aligned} \quad (61)$$

$$M_x = GJ \phi_{,x} - C_1 \phi_{,xxx}$$

The following four stability equations are derived by considering equilibrium of forces and moments

$$\begin{aligned} EA u_{,xx}^0 + N_{xyR}^{(k)} - N_{xyL}^{(k)} &= 0 \\ EI_{zz} v_{,xxxx}^0 + EI_{yz} w_{,xxxx}^0 + \bar{P} [v_{,xx}^0 + z_O \phi_{,xx}^{(k)}] \\ -N_{yyR}^{(k)} + N_{yyL}^{(k)} - Y_R N_{xyR,x}^{(k)} + Y_L N_{xyL,x}^{(k)} &= 0 \\ EI_{yz} v_{,xxxx}^0 + EI_{yy} w_{,xxxx}^0 + \bar{P} [w_{,xx}^0 - y_O \phi_{,xx}^{(k)}] \\ -V_{yR}^{(k)} + V_{yL}^{(k)} - z_R [N_{xyR,x}^{(k)} - N_{xyL,x}^{(k)}] &= 0 \\ C_1 \phi_{,xxxx}^{(k)} - [GJ - (EI_O/EA) \bar{P}] \phi_{,xx}^{(k)} + \bar{P} [z_O v_{,xx}^0 - y_O w_{,xx}^0] \\ + (z_R - z_O) [N_{yyR}^{(k)} - N_{yyL}^{(k)}] - (Y_R - Y_O) V_{yR}^{(k)} + (Y_L - Y_O) V_{yL}^{(k)} \\ + M_{yyR}^{(k)} - M_{yyL}^{(k)} + (\bar{\omega}_S - \omega_R) N_{xyR,x}^{(k)} - (\bar{\omega}_S - \omega_L) N_{xyL,x}^{(k)} &= 0 \end{aligned} \quad (62)$$

The expressions for the constraint forces and moments, equations (52) and (60), may be substituted in equations (62) to yield a new set of equations for the k^{th} stiffener. This new set of equations will involve the buckling displacements and twist of the adjacent stiffeners as well as those of the stiffener under consideration.

Buckling displacements are assumed in the form

$$\begin{aligned} u^o(k) &= U^* \cos \bar{n}x \\ v^o(k) &= V^* \sin \bar{n}x \\ w^o(k) &= W^* \sin \bar{n}x \\ \phi(k) &= \Phi^* \sin \bar{n}x \end{aligned} \quad (63)$$

Equations (62) may now be written in the form

$$[AA] \begin{Bmatrix} U^* \\ V^* \\ W^* \\ \Phi^* \end{Bmatrix} = \bar{P} [BB] \begin{Bmatrix} V^* \\ W^* \\ \Phi^* \end{Bmatrix} = 0 \quad (64)$$

In the above [AA] is of order $4N \times 4N$ and [BB] is of order $4N \times 3N$. By eliminating the column submatrix $\{ U^* \}$ a standard eigenvalue problem of order $3N \times 3N$ is obtained.

$$[\bar{AA}] \begin{Bmatrix} V^* \\ W^* \\ \Phi^* \end{Bmatrix} = \bar{P} [\bar{BB}] \begin{Bmatrix} V^* \\ W^* \\ \Phi^* \end{Bmatrix} \quad (65)$$

The lowest eigenvalue, \bar{P}_{cr} , corresponds to the stiffener buckling load.

SKIN/STIFFENER INTERFACE STRESSES

When the panel is subject to internal pressure loads or has a buckled skin and when the panel stiffeners are bonded or cocured to the skin, the critical failure mode may involve separation of the skin and stiffener. Prior to separation, the interface between the skin and stiffener attains a complex stress distribution. This distribution of stresses may include longitudinal and transverse direct stresses, σ_x and σ_y , normal direct stress, σ_z , inplane shear stress, τ_{xy} , and transverse shear stresses, τ_{xz} and τ_{yz} .

The interface stress analysis in POSTOP is an attempt to provide the designer with a means of minimizing the tendency toward skin/stiffener separation. Prevention of this mode from being critical, rather than prediction of the separation failure load, is the objective of the current analysis. The computational efficiency required of any analysis in a practical sizing code is a strong constraint on the types of analyses which may be included in such codes. This requirement excluded from consideration any highly non-linear separation failure analysis.

The current interface stress analysis provides an efficient, closed-form solution for the interface stresses based on the assumption of elastic linear material behavior and small deflections. Margins of safety are obtained with the Tsai-Hill's criterion as applied to a three dimensional stress state.

The physical model for which the solution is developed is shown in Figure 10. The model consists of flange and skin plates and an interface layer. The attached flanges are assumed to be of equal width b and equal uniform thickness, t_f . The remainder of the stiffener is replaced by a vertical and a rotational spring in the web midplane having stiffnesses k_z and k_r , respectively. The skin between stiffener flange edges is replaced by equivalent moments and shear forces in the buckled skin. These stress resultants are distributed sinusoidally over the buckled skin wavelength, λ . A transverse stiffness k_y , representing the transverse membrane stiffness of the removed skin, acts on the edges of the remaining skin plate. Longitudinal inplane loads are present in the flange and skin and a transverse inplane load in the skin. Inplane shear is currently not

included in the model. The effect of in plane shear is, however, included in determining the buckled skin equivalent moments, M , and shear forces, V , applied to the skin portion of the model as shown in Figure 10.

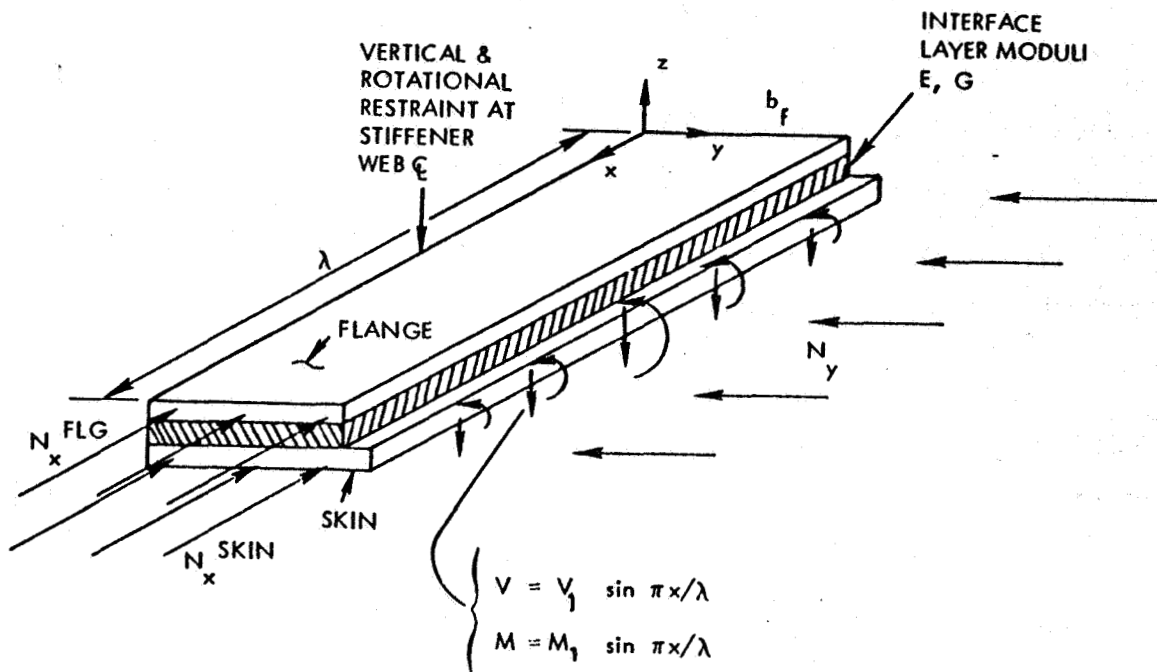


Figure 10. Skin/Stiffener Interface Model

Independent solutions have been developed for the antisymmetric conditions present in postbuckled biaxially loaded panels and for the symmetric condition that results from pressure loading. The antisymmetric case closely approximates the deformation of postbuckled panels loaded with biaxial plus shear loads if the shear load is of a secondary nature as previously assumed and the flange width, b_f , is small relative to the wavelength. Since the solutions are linear, superposition is used to obtain total stresses if required. The interface normal stress, σ_z , and transverse shear stresses, τ_{xz} and τ_{yz} , are obtained directly. The remaining interface stresses are obtained from the skin inplane strains and the requirement of skin-interface compatibility.

The solution procedure for the antisymmetric case is summarized below. The procedure for the symmetric solution is similar.

If the flange and skin are orthotropic and loaded antisymmetrically about the web midplane, they will deform antisymmetrically. The applied

moment and shear may be represented in series form as

$$M(\xi) = \sum_m M_m \sin m\pi\xi$$

$$V(\xi) = \sum_m V_m \sin m\pi\xi$$

in which $m = 1, 2, \dots$ and $\xi = x/\lambda$. The skin displacements in the x , y , and z directions may be written in series form as

$$\begin{aligned} u &= \sum_m \sum_n U_{mn} P_{n+1}(\eta) \cos m\pi\xi \\ v &= \sum_m \sum_n V_{mn} P_n(\eta) \sin m\pi\xi \\ w &= \sum_m \sum_n W_{mn} P_{n+1}(\eta) \sin m\pi\xi \end{aligned} \quad (67)$$

in which $n = 0, 2, 4, \dots$ and $\eta = y/b_f$. The $P_n(\eta)$ are Legendre polynomials. The interface stresses acting on the upper surface of the skin may be written in similar form

$$\begin{aligned} \tau_{xz} &= \sum_m \sum_n p_{xmn} P_{n+1}(\eta) \cos m\pi\xi \\ \tau_{yz} &= \sum_m \sum_n p_{ymn} P_n(\eta) \sin m\pi\xi \\ \sigma_z &= \sum_m \sum_n q_{mn} P_{n+1}(\eta) \sin m\pi\xi \end{aligned} \quad (68)$$

A weighted residual procedure is used to establish the governing equations for the inplane and transverse displacements of an orthotropic plate subject to surface normal and tangential loads representing interface stresses. Biaxial inplane loads are included in the governing equations. Substitution of the series expressions for the applied edge moments and shears, the skin displacements, and the interface stresses into the governing equations yields a set of linear algebraic equations

for the displacement coefficients as functions of the applied edge load and unknown surface load coefficients. In matrix form these equations are

$$\begin{bmatrix} a & | & b \\ \hline c & | & d \end{bmatrix} \begin{Bmatrix} U \\ \hline V \end{Bmatrix} = \begin{bmatrix} e & | & o \\ \hline o & | & f \end{bmatrix} \begin{Bmatrix} P_x \\ \hline P_y \end{Bmatrix} \quad (69)$$

$$\begin{bmatrix} g \end{bmatrix} \begin{Bmatrix} W \end{Bmatrix} = \begin{bmatrix} h & | & r & | & s \end{bmatrix} \begin{Bmatrix} p_x \\ \hline p_y \\ \hline q \end{Bmatrix} + \begin{Bmatrix} \bar{M} \end{Bmatrix} + \begin{Bmatrix} \bar{V} \end{Bmatrix}$$

in which the terms of the coefficient matrices are functions of the plate stiffnesses and dimensions. Due to the properties of the Legendre polynomials chosen as the shape functions, these terms may be rapidly computed. The $\{\bar{M}\}$ and $\{\bar{V}\}$ are functions of the applied edge loads. If N shape functions are included in the series expressions, equations (69) contain $3N$ equations. These equations may be developed independently for each value of m as required by the series expressions of the edge loads, equations (66). Similarly, a set of equations may be developed for the flange displacements u_f, v_f, w_f .

$$\begin{bmatrix} \bar{a} & | & \bar{b} \\ \hline \bar{c} & | & \bar{d} \end{bmatrix} \begin{Bmatrix} U^f \\ \hline V^f \end{Bmatrix} = \begin{bmatrix} \bar{e} & | & o \\ \hline o & | & \bar{f} \end{bmatrix} \begin{Bmatrix} p_x \\ \hline p_y \end{Bmatrix} \quad (70)$$

$$\begin{bmatrix} \bar{g} \end{bmatrix} \begin{Bmatrix} W^f \end{Bmatrix} = \begin{bmatrix} \bar{h} & | & \bar{r} & | & \bar{s} \end{bmatrix} \begin{Bmatrix} p_x \\ \hline p_y \\ \hline q \end{Bmatrix}$$

The two plates are forced to have compatible deformations through the continuity conditions

$$\begin{aligned} u_f &= u - \frac{1}{2} (t_f + t_s) \frac{\partial w}{\partial x} + \tau_{xz} t_a / G - (\frac{1}{2} t_f t_a / E) \frac{\partial \sigma_z}{\partial x} \\ v_f &= v - \frac{1}{2} (t_f + t_s) \frac{\partial w}{\partial y} + \tau_{yz} t_a / G - (\frac{1}{2} t_f t_a / E) \frac{\partial \sigma_z}{\partial y} \\ w_f &= w + (t_a / E) \sigma_z \end{aligned} \quad (71)$$

in which t_f, t_s , and t_a are the flange, skin, and interface thicknesses, respectively, and E and G are the elastic moduli of the interface layer.

If equations (69) and (70) are solved for the displacement coefficients and substituted, along with equations (67) and (68), into the continuity conditions, equations (71), a set of 3N linear algebraic equations for the interface stress coefficients results

$$[A] \begin{Bmatrix} p_x \\ p_y \\ q \end{Bmatrix} = [B] \begin{Bmatrix} \bar{M} \\ \bar{V} \end{Bmatrix} \quad (72)$$

These equations may be developed and solved for each value of m in the edge load series yielding the interface stress coefficients. The interface stresses are then obtained from equations (68).

The interface stresses are evaluated at a number of points on a grid defined by the program user. Typically points along the flange edge will be critical although locations near the web may be critical in some cases. Some examples are given in the User's Manual, Reference 4.

Margins of safety at the grid points are computed according to the Tsai-Hill criterion. This criterion may be written as

$$\begin{aligned} S = & \left(\frac{\sigma_x}{\bar{\sigma}_x} \right)^2 + \left(\frac{\sigma_y}{\bar{\sigma}_y} \right)^2 + \left(\frac{\sigma_z}{\bar{\sigma}_z} \right)^2 - \sigma_x \sigma_y \left(\bar{\sigma}_x^{-2} + \bar{\sigma}_y^{-2} - \bar{\sigma}_z^{-2} \right) \\ & - \sigma_x \sigma_z \left(\bar{\sigma}_x^{-2} + \bar{\sigma}_z^{-2} - \bar{\sigma}_y^{-2} \right) - \sigma_y \sigma_z \left(\bar{\sigma}_y^{-2} + \bar{\sigma}_z^{-2} - \bar{\sigma}_x^{-2} \right) \\ & + \left(\frac{\tau_{xy}}{\bar{\tau}_{xy}} \right)^2 + \left(\frac{\tau_{xz}}{\bar{\tau}_{xz}} \right)^2 + \left(\frac{\tau_{yz}}{\bar{\tau}_{yz}} \right)^2 < 1 \end{aligned} \quad (73)$$

in which the bar superscript denotes allowable stresses. Different allowables may be specified for tensile and compressive direct stresses. The allowable stresses appropriate to the sense of the computed stresses

are used in computing the values of S at the grid points. The margin of safety in this mode is $1/\sqrt{S} - 1$.

The inplane interface stresses used in equation (73) are

$$\sigma_x = \frac{E}{1 - \nu^2} (\epsilon_x + \nu \epsilon_y)$$

$$\sigma_y = \frac{E}{1 - \nu^2} (\nu \epsilon_x + \epsilon_y)$$

$$\tau_{xy} = G \gamma_{xy}$$

in which ϵ_x is the longitudinal strain at the interface midsurface. The strains ϵ_y and γ_{xy} are conservatively set equal to the skin transverse and shear strains, respectively.

SKIN LAYUP DESIGN CONSTRAINTS

It is often desirable to place constraints on the proportions of skin material oriented in various directions. For example, the "soft skin" concept has been used as a means of enhancing the damage tolerance of stiffened panels. In this case the skin is required to have a high proportion, say 60 percent or higher, of its total material oriented in the ± 45 -degree directions. Without a lower bound on the proportion of ± 45 -degree material, the sizing procedure would most likely result in less than 60 percent ± 45 -degree material in the skin.

To achieve designs such as the soft skin concept, lower bounds may be placed on the proportions of skin material oriented in three general directions or zones as shown in Figure 11, Zone 1, the longitudinal zone, is defined as the x -direction (stiffener direction), plus or minus a small angle $\bar{\theta}$. The angle $\bar{\theta}$ may be zero or any small positive number of degrees. Zone 3, the transverse zone, is defined as the y -direction plus or minus $\bar{\theta}$. Zone 2, the intermediate zone, includes directions excluded from Zones 1 and 3. To achieve the soft skin design described above, lower bounds of

0.0, 0.6 and 0.0 would be set for Zones 1, 2, and 3, respectively, and $\bar{\theta}$ would be set to zero degrees. The purpose of the angle $\bar{\theta}$ is to allow slightly off-axis, say ± 5 -degree, material to be used as the basic longitudinal material rather than only zero-degree material. Transverse material would, in this case, be $\pm(85/95)$ -degree material and $\bar{\theta}$ would be set at 5-degrees. If no skin layup design constraints are desired, all lower bounds are simply set to zero.

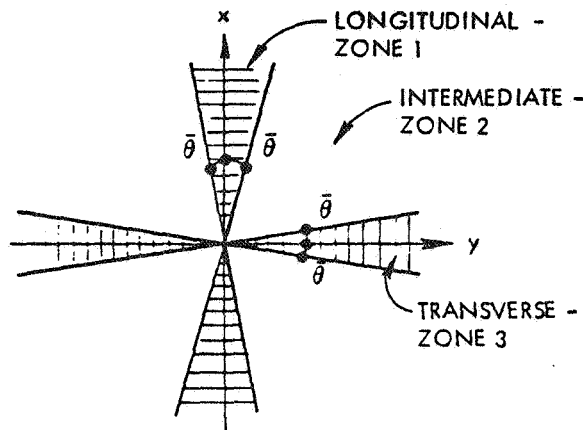


Figure 11. Skin Layup Design Constraint Zones for Skin Material Orientations

MULTIPLE LOAD CASES

POSTOP has the capability to analyze or size panels with up to five separate load cases. In the sizing mode, a minimum-weight panel is obtained that satisfies all design requirements for all the load cases. The margins of safety for each failure mode in each load case are computed and the critical margins of safety are used to formulate design constraints during sizing.

Each load case has its own inplane and normal loads, eccentricities, temperature, required panel stiffnesses, skin buckling requirement, material properties and allowables and strain limitations. Stiffener dimensions and spacing, laminate configurations, and skin layup design constraints are common to all load cases.

SIZING

The determination of values for the panel variables so that all margins of safety are within prescribed bounds and the panel has the lowest possible weight is referred to as sizing. POSTOP uses the program CONMIN (Reference 2) to determine how the variables should be changed from an initial design. The program COPES (Reference 1) is used to impose limits on the variables or margins to safety, to link variables, and to provide design aids such as the sensitivity study option or the approximate optimization techniques described in this reference. COPES also provides the ability to size a panel to meet objectives other than minimum weight. For example, a panel with a given weight could be sized to provide a maximum positive margin of safety in a particular failure mode. The margins of safety are computed in all cases by the analysis routines previously discussed.

OPTIMIZATION PROBLEM STATEMENT

The standard statement of an optimization problem is: Find the values for the design variables X_i such that some objective function $Y(X_i)$ is minimized subject to the constraints $G_j(X_i) \leq 0$ and $(\text{Lower Bound})_i \leq X_i \leq (\text{Upper Bound})_i$.

Normally the objective function is the panel weight per unit plan form area. Alternatively any margin computed by the analysis routines may be chosen as the objective function in which case $Y(X_i) = -MS_j$. The design variables may include any of the stiffener flange widths, the stiffener height, the stiffener spacing and thicknesses of the various laminae defining the stiffener and skin laminates. Panel length is normally held constant but may be chosen as a variable if desired.

COPES allows upper and lower bounds to be placed on the variables or any function of the variables. Variable constraints are treated as linear side constraints. Function constraints may be linear or nonlinear. In POSTOP the user defines bounds on all variables and margins. Panel weight may also be bounded in a margin maximization sizing. The constraints

$G_j(X_j)$ may be expressed in standard form as

$$\text{Lower Limit} - \text{Value} = G_i(X_i) \leq 0$$

$$\text{Value} - \text{Upper Limit} = G_k(X_i) \leq 0$$

COPES internally formulates the constraints in this way. Normally each margin of safety will be required to be greater than zero, or some minimum value, and will not have an upper limit imposed. In this way different margins of safety may be required to have different minimum values. Variables must be constrained to have positive values. These side constraints are imposed directly by limiting possible values that the variables can assume.

OPTIMIZATION PROCEDURE

The nonlinear mathematical programming procedure used in CONMIN is a modification of the method of feasible directions (Reference 3). This procedure is well documented in Reference 2 and only a brief overview is given here.

A starting design is defined which may be in the feasible or infeasible region but should be "reasonable." Gradients to $Y(X_i)$ and the critical $G_j(X_i)$ are computed. POSTOP requires CONMIN to compute the gradients by finite differences since most of the margins of safety are computed by algorithms rather than explicit functions. Assuming the starting design to be feasible, it is modified using the conjugate directions method until a constraint is encountered. Further modifications are made in a direction that will decrease $Y(X_i)$ but not violate the $G_j(X_i)$. When no further modifications are possible the optimum design has been found. A global optimum cannot be assured. Different starting designs may be used to achieve some confidence as to the global or local nature of the optimum designs. In most cases starting designs that are well within the feasible region allow the optimization procedure to produce designs that are very close to the apparent global design. Experience with POSTOP has shown that local minimum values of panel weight may be found that are approximately equal, but the corresponding designs may be significantly different.

REFERENCES

1. Madsen, Leroy E. and Garret N. Vanderplaats, "COPES - A Fortran Control Program for Engineering Synthesis," Report No. NPS69-81-003, Naval Postgraduate School, Monterey, Calif., March 1982.
2. Vanderplaats, Garret N., "CONMIN - A Fortran Program for CONstrained Function MINimization - User's Manual," NASA TM X-62,282, 1973.
3. Zoutendijk, G., Methods of Feasible Directions, Elsevier Publishing Co., Amsterdam, 1960.
4. Biggers, Sherrill B. and John N. Dickson, "POSTOP: Postbuckled Open-STiffener Optimum Panels - User's Manual," NASA CR-172260, January 1984
5. Timoshenko, S. P., and Gere, J. M., "Theory of Elastic Stability," Second Edition, McGraw-Hill Book Company Inc., 1961.
6. Koiter, W. T., "Het Schuifplooiveld by Grote Overschrydingen van de Knikspanning," National Luchtvaart Laboratorium, Report S 295, November 1946, in Dutch.
7. Bushnell, David, "Panel Optimization with Integrated Software (POIS), Volume I - PANDA -- Interactive Program for Preliminary Minimum Weight Design," AFWAL-TR-81-3073, July 1981.

1. Report No. NASA CR-172259		2. Government Accession No.		3. Recipient's Catalog No.	
4. Title and Subtitle POSTOP: POSTBUCKLED OPEN-STIFFENER OPTIMUM PANELS -- THEORY AND CAPABILITY				5. Report Date January 1984	
				6. Performing Organization Code	
7. Author(s) J. N. Dickson and S. B. Biggers				8. Performing Organization Report No.	
9. Performing Organization Name and Address Lockheed-Georgia Company 86 South Cobb Drive Marietta, GA 30063				10. Work Unit No.	
				11. Contract or Grant No. NAS1-15949	
				13. Type of Report and Period Covered Contractor report	
12. Sponsoring Agency Name and Address National Aeronautics and Space Administration Washington, DC 20546				14. Sponsoring Agency Code	
15. Supplementary Notes Langley Technical Monitor: Dr. James H. Starnes					
16. Abstract The computer program POSTOP has been developed to serve as an aid in the analysis and sizing of stiffened composite panels that may be loaded in the postbuckling regime. A comprehensive set of analysis routines has been coupled to a widely used optimization program to produce this sizing code. POSTOP is intended for the preliminary design of metal or composite panels with open-section stiffeners, subjected to multiple combined biaxial compression (or tension), shear and normal pressure load cases. Longitudinal compression, however, is assumed to be the dominant loading. Temperature, initial bow eccentricity and load eccentricity effects are included. The panel geometry is assumed to be repetitive over several bays in the longitudinal (stiffener) direction as well as in the transverse direction. Analytical routines are included to compute panel stiffnesses, strains, local and panel buckling loads, and skin/stiffener interface stresses. The resulting program is applicable to stiffened panels as commonly used in fuselage, wing, or empennage structures. This report describes in some detail the analysis procedures and rationale for the assumptions used therein. A brief description of the sizing methodology is given. Detailed instructions for the use of the code and interpretation of the output from the program are given in a separate User's Manual (NASA CR-1722-60).					
17. Key Words (Suggested by Author(s)) Postbuckling, Stiffened Panels, Composites, Sizing Code, Analysis Methods			18. Distribution Statement Unclassified - Unlimited Subject Category 39		
19. Security Classif. (of this report) Unclassified	20. Security Classif. (of this page) Unclassified	21. No. of Pages 50	22. Price A03		